SHORT-TERM SAMPLING SPACE OPTIMIZATION

*J. L. Machado[1], R. S. Leal[1], V. C. Koppe[1] and R. L. Peroni[1], L.N. Capponi[2]

[1] *Federal University of Rio Grande do Sul – UFRGS. Mining Engineering Department*
Avenida Bento Gonçalves, 9500, Bloco IV Prédio 75
Porto Alegre, RS, Brasil.
(*Corresponding author: jaquelepkoski@gmail.com)

[2] *Vale Fertilizantes S.A.*
Rodovia MG - 341, Km 25.
Tapira, MG, Brasil

24th World Mining Congress
MINING IN A WORLD OF INNOVATION
October 18-21, 2016 • Rio de Janeiro /RJ • Brazil

SHORT-TERM SAMPLING SPACE OPTIMIZATION

ABSTRACT

The sampling spatial distribution and procedures have a pronounced influence on the geological modeling, grade estimates, resources classification and mine planning. The collection, preparation and analysis of samples are time consuming and also expensive. Therefore, the sampling strategy must be carefully planned. The short-term sampling is a solid contribution to improve knowledge about the geological contacts and to promote the grade control from the mining operation perspective. The geostatistical analysis provides useful tools to define optimal sampling location in the short-term, avoiding lack or excess of sampling to be collected and analyzed. Insufficient samples affect grade estimations, generating values with low confidence to be assigned into the blocks. On the other hand, excess of samples generates unnecessary costs and time consumption for their preparation and analysis, which may contribute for delays during the grades model updating and consequently affect the decision making process. This work aims to demonstrate an application of a methodology to determine the optimal drill spacing for short-term purposes, using geostatistical simulation to assess the uncertainty and measure the benefit of cutting down and/or adding samples to certain areas. The techniques are tested in a phosphate deposit to find a representative grid that allows one to obtain suitable grade estimates for each block to improve the short-term mine planning.

KEYWORDS

MINE PLANNING, SAMPLING OPTIMIZATION, SHORT-TERM, GEOSTATISTICS, SIMULATION.

INTRODUCTION

The application of standardized sampling techniques helps all the subsequent stages of mining, such as, but not limited, to block model estimation, mine planning and processing. Therefore, the use of an accurate sampling protocol is essential for a better performance and accuracy of all the subsequent steps. Moreover, oversampling should also be avoided due to the high costs attached to the sampling tasks. For this reason, obtaining a suitable sample mesh becomes an essential, but not always obvious duty. In short-term operational scenario, it is important the sample collection and analysis to be efficient, so there is time to take necessary decisions in short periods.

Some authors use uncertainty measures to optimize sample patterns and/or drill spacing in a long-term scenario for resources and reserves classification. Koppe (2011) used uncertainty measures to locate new drillings on a regular grid of samples in order to reduce risk in a given transfer function. The author also mentions that the uncertainty level of a function that reflects the uncertainty of one or more geological attributes can be used in a mineral resource classification. The scenarios generated by stochastic simulation can also be used to analyze the uncertainty associated with the values of a global transfer function. When the transfer function is the ore tonnage above a given cut-off grade, each simulated scenario results in a value for ore tonnage and the uncertainty associated with this tonnage can indicate the reserves classification as probable or proven.

Emery et. al. (2009) used an optimization algorithm to find the sampling pattern that minimizes the average error from geostatistical simulation. The error depends on the ore variability, in a way that more samples provide better accuracy in the grade estimation. The minimum number of additional samples depends on the sampling objective (Koppe, 2011). In a short-term scenario, it is desired to collect a minimum number of samples to reduce costs and time.

Reducing the grade variability in processing plant feeding is fundamental, especially when the grades are low and there are contaminants. Geostatistical techniques, such as Ordinary Kriging and Indicator Kriging allow the construction of estimated models. However, these techniques do not give access to uncertainty and smooth the natural variance of the original data. Geostatistical simulation, on the other hand, allows to access the average error of the estimation for a better decision making process. This study aims to minimize the error by testing the effect of short-term samples spacing, comparing different sampling grids. The grid that shows higher spacing and minimize the error to an acceptable level will be considered optimal. The simulation algorithm used in this case study was Turning Bands (Matheron, 1973).

The first step is the simulation performance for the available data. Then, a simulated scenario is chosen as reference to obtain data with different spacing. The simulation algorithm is performed again for several spacing, and the uncertainty about the estimated concentrations is measured by the error calculation. Finally, the impact on the uncertainty by different data spacings is evaluated. This case study used data from a phosphate mine in Minas Gerais - Brazil.

Case Study

The methodology was tested using a short-term database, comprised by 299 rotary diamond drill holes, drilled in a regular grid of 25 m x 25 m, with different orientations according the geological zones. The holes have in average 35 m depth and the length of samples is standardized at 5 m.

The procedure was used to sample the main variable of interest, the apatite content (P_2O_5), in a specific region of the mine. In this region there are 650 samples, with average grade of 6% and variance of 4.75%². Figure 1 shows the plan view of the selected holes and the color legend for the P_2O_5 grades (a) and the histogram for the original data (b).
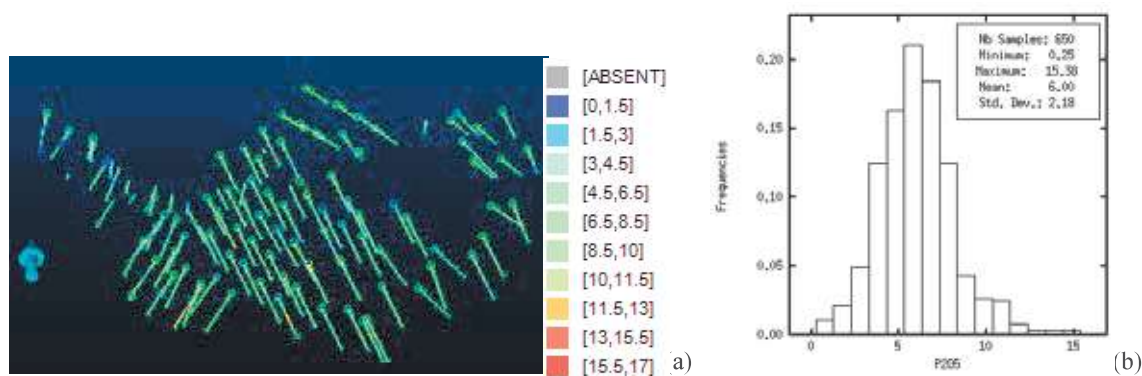

Figure 1. Sample location and original dataset histogram, respectively.

In Turning Bands the simulated values are derived from a distribution based on the associated theory with multi Gaussian random functions. The normalization of a distribution is generated from a function that can be graphically generated as shown in Figure 2, where the values corresponding to the p-quantile of the original

cumulative data distribution are correlated with the corresponding values in the normal space. The histogram of the normalized data (Figure 3) follows a Gaussian distribution, with mean of zero and standard deviation of 1.
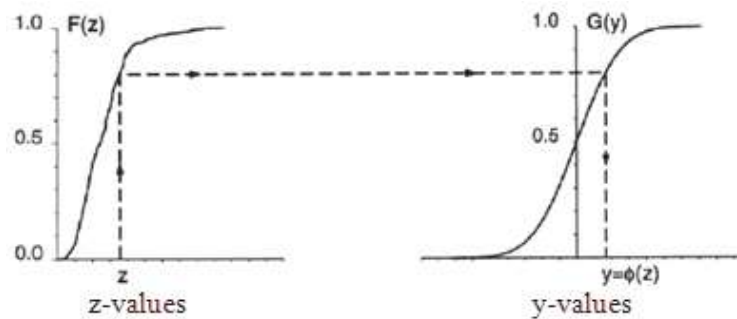

Figure 2. Process data standardization. Source: Goovaerts, 1997 – pp. 268.

After the data normalization (the histogram of original data normalized is presented on Figure 3), the analysis of the spatial continuity was performed using variograms. The variogram model of normalized data was inferred from the original data variogram model, as it has the same spatial continuity characteristics as the original data.
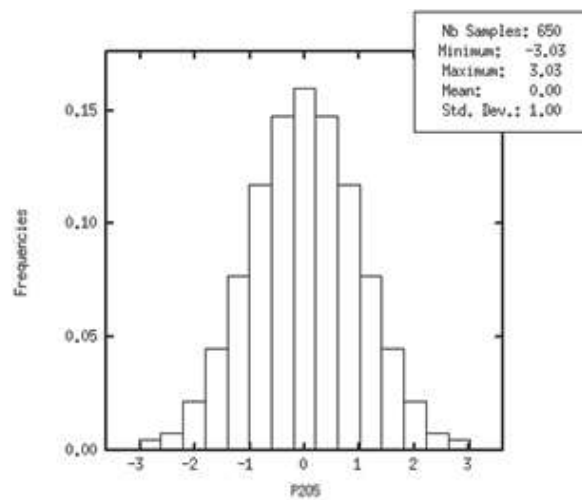
Figure 3. P_2O_5 normalized data histogram.

The variogram models may be seen in Figure 4 and the variogram equation can be seen in Equation (1). The variograms of P_2O_5 presented higher continuity in azimuth N67 with a 200 m approximately range.
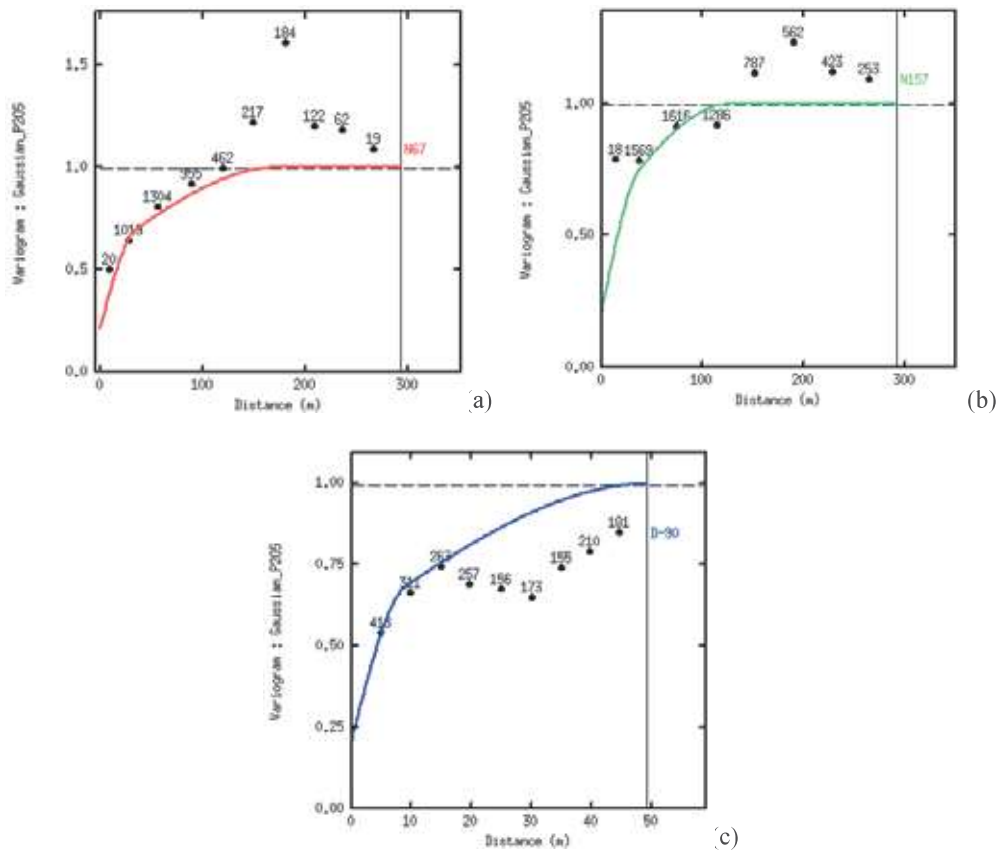
Figure 4. P$_2$O$_5$ standardized variograms in 3 directions. (a) major continuity direction (N67), (b) median continuity direction (N157), (c) minor continuity direction (D90). Continuous line represent the variogram model and dots represent the experimental variograms.

$$\gamma(h) = 0.2105 + 0.3579 \times Sph\left(\frac{N_{67}}{35} + \frac{N_{157}}{30} + \frac{vert}{9}\right) + 0.4316 \qquad (1)$$
$$\times Sph\left(\frac{N_{67}}{175} + \frac{N_{157}}{100} + \frac{vert}{50}\right)$$

The simulation was performed on small support scale (quasi-punctual) with grid spacing of 2m x 2m x 5m in the X, Y and Z, respectively, using the normalized data. The search parameters used in the simulation were the same as the scope of the continuity model in each direction. In total, 80 realizations for P$_2$O$_5$ grade were generated using Turning Bands simulation in the Gaussian space, and then back transformed to the original distribution.

The scenarios obtained by simulation must reproduce the histogram and variogram models of the original data, to validate the simulation. Figure 5 shows the variograms in three directions (colored lines), presenting ergodic fluctuations around the original data model (black lines).
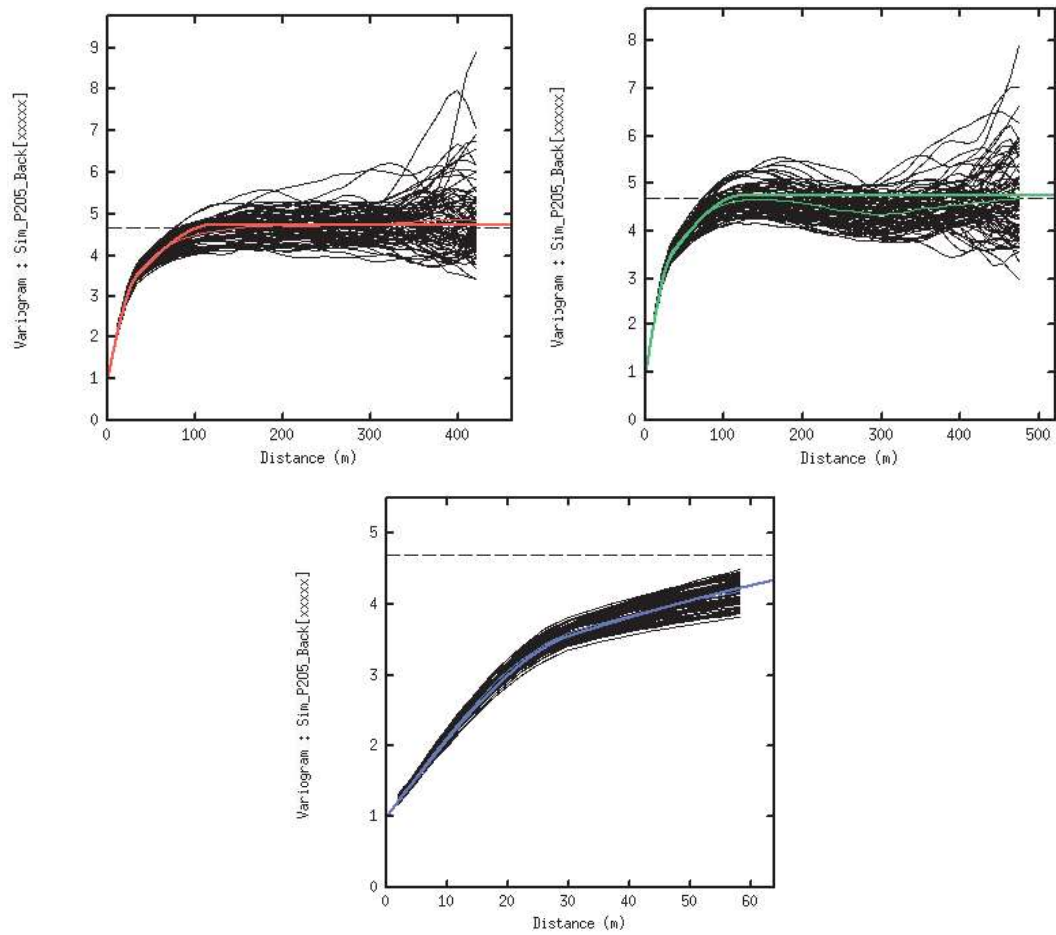
Figure 5. Experimental variograms for the 80 realizations (black lines) and variogram model's input to the simulation algorithm (colored lines).

The maps and histograms for the realizations with lowest, highest variance and the variance closest to the median are shown in Figure 6, Figure 7 and Figure 8, respectively.
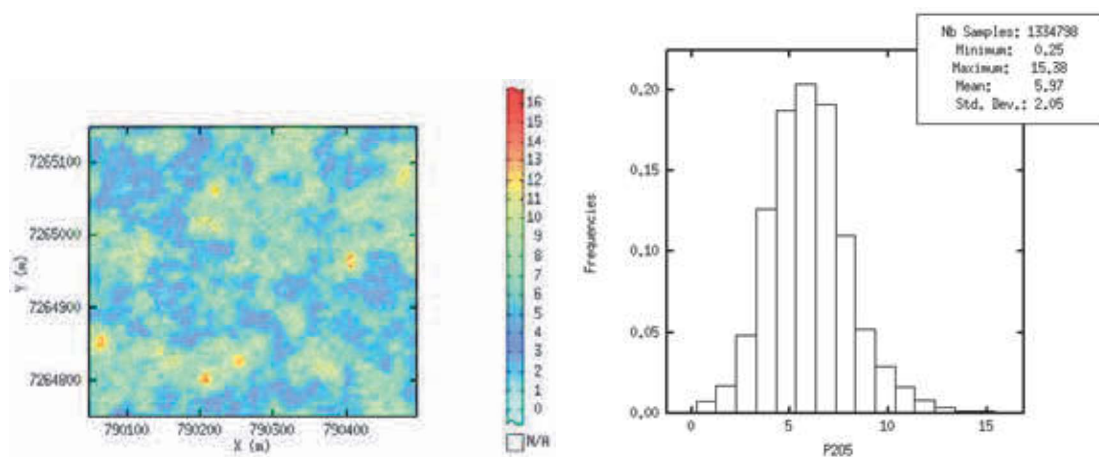

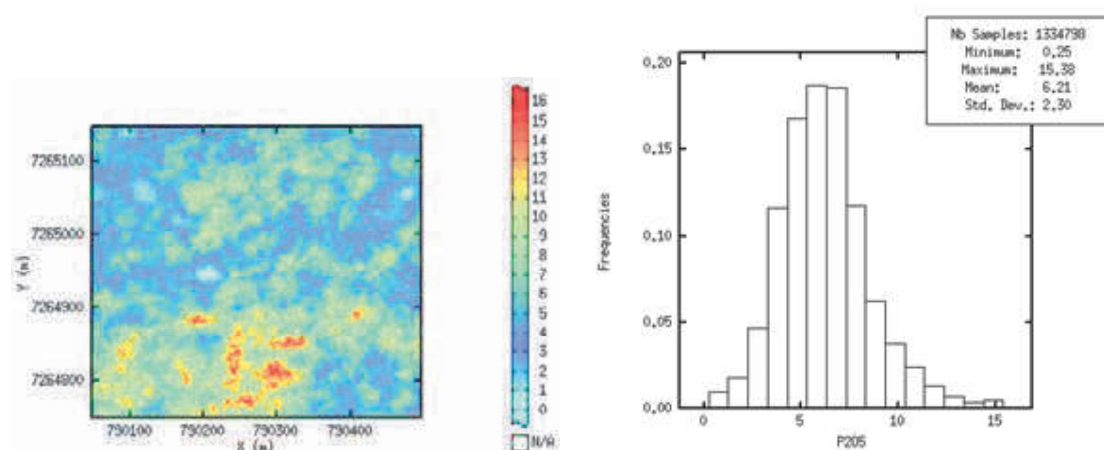Figure 6. Map and histogram for the scenario with lowest variance.

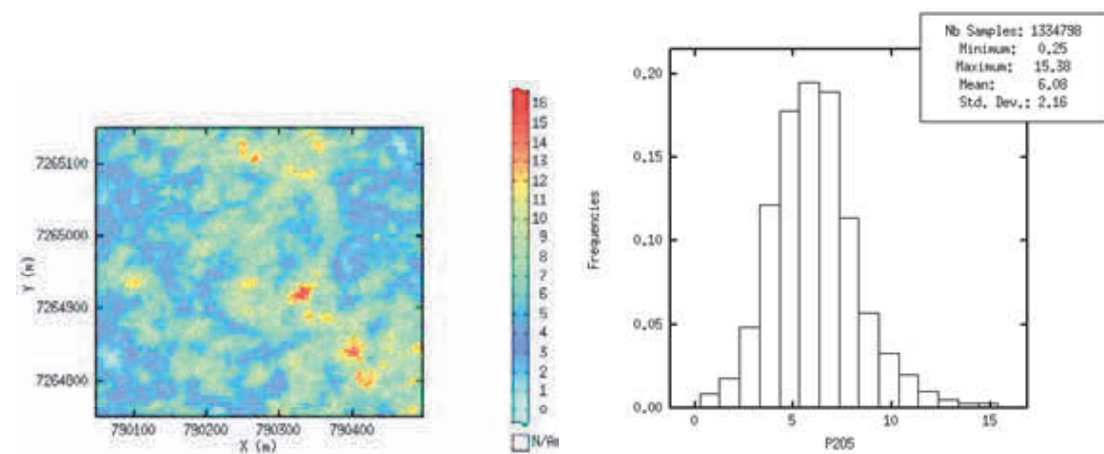Figure 7. Map and histogram for the scenario with highest variance

Figure 8. Map and histogram for the scenario with the variance closest to the median.

Table 1. Statistics for realizations in points support.

	Minimum (% P_2O_5)	Maximum (% P_2O_5)	Mean (% P_2O_5)	Variance (%² P_2O_5)
	0.25	15.38	5.97	4.21
Realization	0.25	15.38	6.08	4.68
	0.25	15.38	6.21	5.28

From the simulated data in each realization were calculated the P_2O_5 grades for 25,524 blocks of 10m x 10m x 10m in the X (east), Y (north), and Z (vertical) directions. The value of each block is the arithmetical average of the previously simulated points within these blocks.

The grid used for the simulation (2m x 2m x 5m) ensured that the distribution of the blocks presented theoretical variance to the variance of blocks (2,54% ²), considering the ergodic fluctuations, which simply means

that the number of simulated points within each block is considered sufficient (for the study 50 simulated points were considered). Table 2 shows statistics for realizations with lowest, highest and the variance closest to the median values for the P_2O_5 in the support block.

Table 2. Statistics for realizations in 10m x 10m x 10m support blocks.

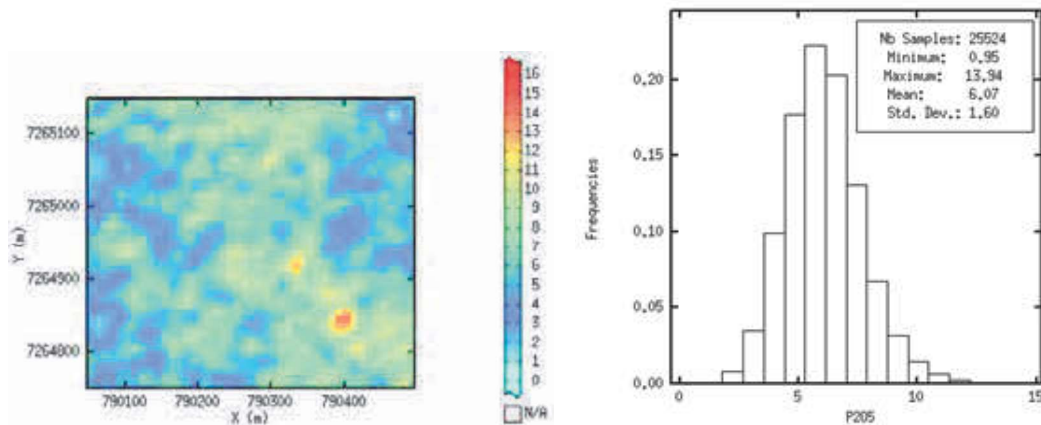|	Minimum (% P_2O_5)	Maximum (% P_2O_5)	Mean (% P_2O_5)	Variance (%² P_2O_5)
Realization	1.46	13.77	5.99	2.16
	0.95	13.94	6.07	2.56
	0.39	14.30	6.21	3.10

Figure 9. Map and histogram for the realization with nearest variance to the median values in blocks support.

Figure 10 shows the standard deviation for several simulated scenarios. The number of scenarios in which the standard deviation becomes stable is considered satisfactory to assess the range of the uncertainty space. Therefore, it is possible to verify that from 60 scenarios this aim is already reached.
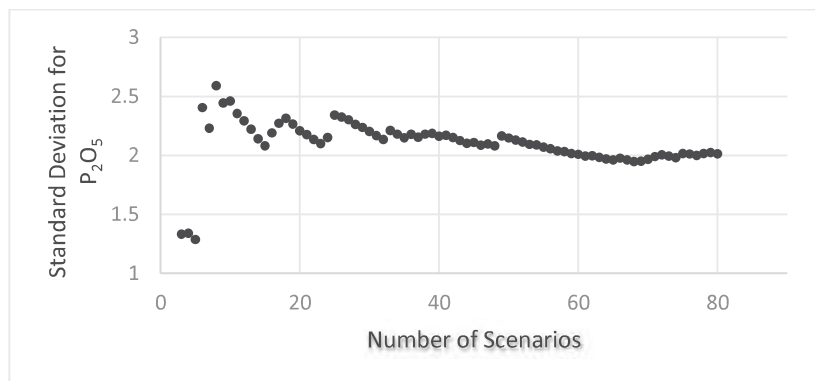

Figure 10. Number of scenarios versus standard deviation of P_2O_5 contents.

Additional Data Obtained From Simulation

Among the 80 simulation scenarios only one was chosen as the reference for the creation of virtual dataset. The reference scenario was the 48th considering it has the closest variance to the median variance of the data, however all scenarios are equiprobable to represent the mineral deposit. Using the realization in points support (2m x 2m x 5m), an interpolation by the nearest neighbor method with a search radius of 0.001 meters at nodes with spacing 6m x 6m x 5m at east, north and vertical direction, respectively. The values interpolated represent the values of samples from a sampling campaign. This procedure created a new dataset with 148,856 samples spaced by of 6m x 6m x 5m.
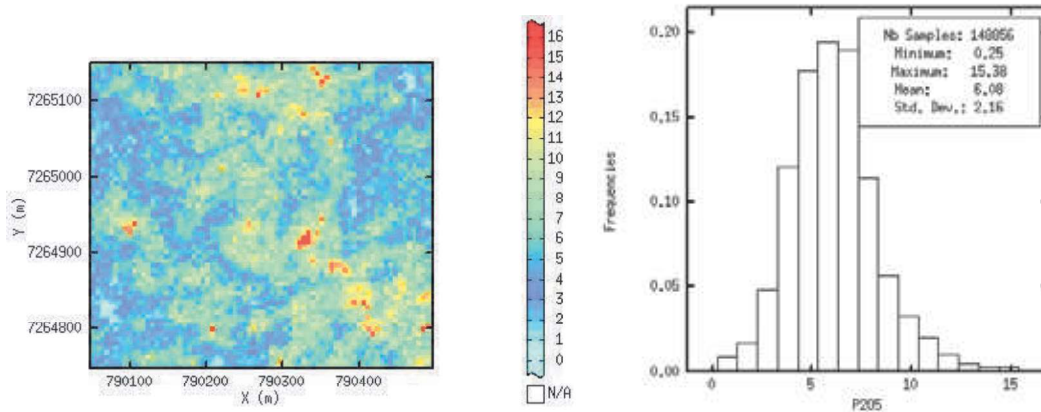

Figure 11. Map and histogram for the new dataset.

These data were normalized, and the variograms were adjusted due to a change in the variance. A new simulation was performed with these data to calculate the new error. From the simulated levels in each realization, the P_2O_5 grade was calculated for 34,200 blocks of 10m x 10m x 10m in the X, Y, and Z directions. The value of each block is the arithmetical average of the points within the blocks.

The result of the simulation provides for each block a distribution probability based on the obtained realizations. The error of the estimate is calculated after the results treatment, by compiling all realizations for each block and their calculation formula is shown in Equation (2), where the Q95 is the quantile 95, Q5 is the quantile 5 and Etype is the average of all scenarios. Equation 2 supposes a distribution of simulated values symmetric around E-type (as illustrated in Figure 12).
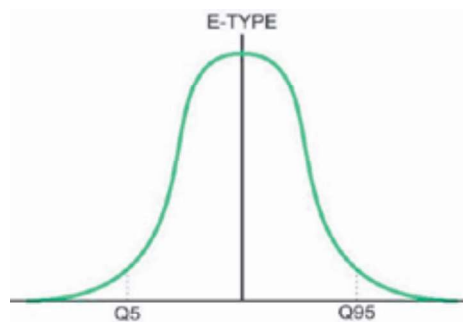
$$Error = \frac{Q95 - Q5}{2 \times Etype} \tag{2}$$

Figure 12. Representation of quantile and E-type realizations.

Based on the information from the mine considered for this case study, an error of 10% about the estimated of each block value can be accepted. With the 6 m x 6 m grid was obtained an average error of 8% for all simulated blocks, which means that when kriging is performed with the data in mesh 6 m x 6 m, the error of the estimated content is 8% higher or lower. Note that this error is an approximation of the maximum error about the estimate of each block.
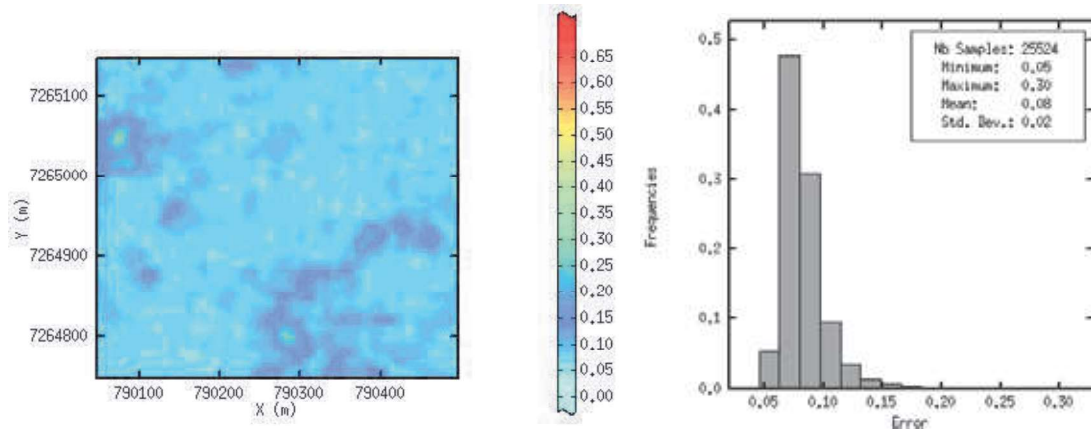

Figure 13. Error map and the histogram to the grid 6m x 6m x 5m.

Using the same methodology, were tested grids with spacing of 10m x 10m, 14m x 14m, 18m x 18m and 22 m x 22m. The results can be seen in Figures 14 to 17.
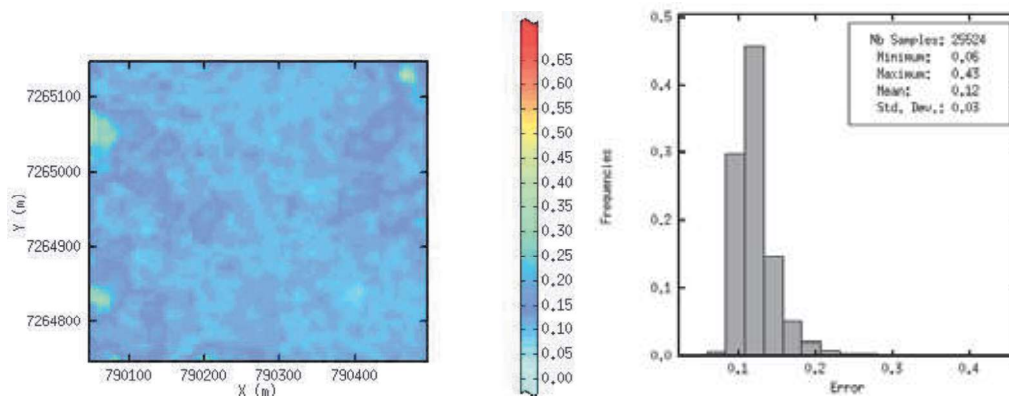

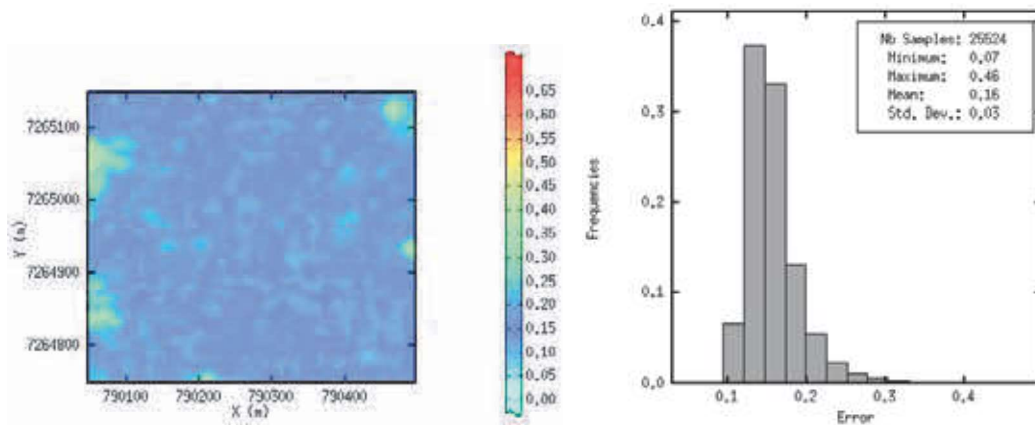Figure 14. Error map and the histogram to the grid 10m x 10m x 5m.

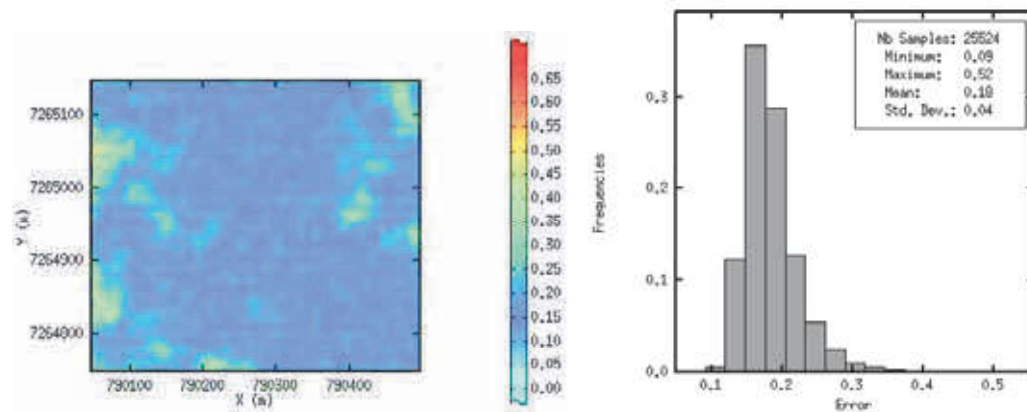Figure 15. Error map and the histogram to the grid 14m x 14m x 5m.

Figure 16. Error map and the histogram to the grid 18m x 18m x 5m.
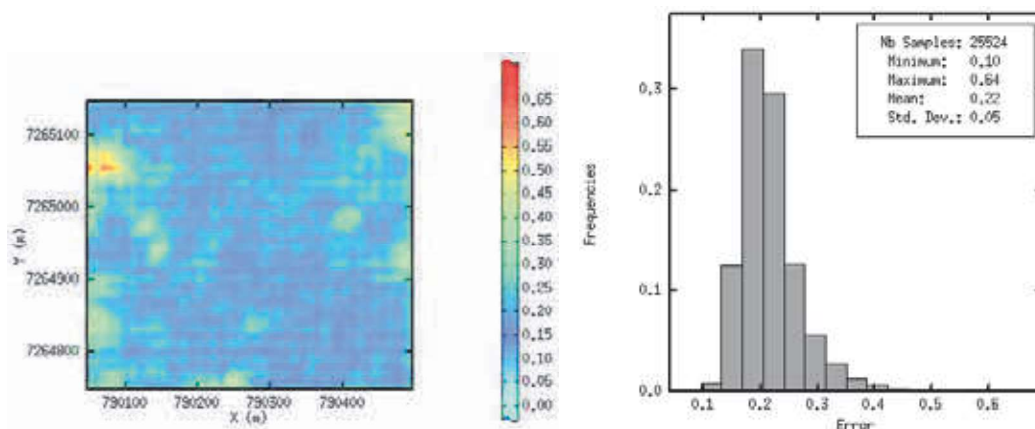

Figure 17. Error map and the histogram to the grid 22m x 22m x 5m.

Figure 18 shows the error obtained for the different grids tested. As can be seen the error increases acoording the sampling density is sparser. With this graph it is possible to select the "optimal" drill hole spacing considering the acceptable error.
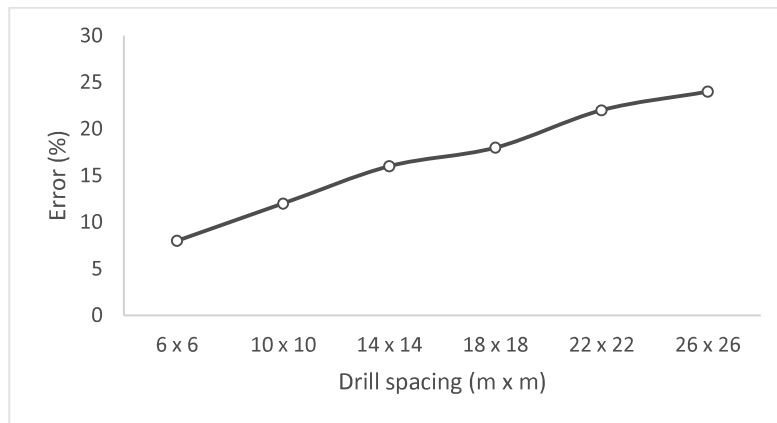
Figure 18. Average error versus drill spacing.

CONCLUSION

The simulation conducted in this study generated 80 equally probable scenarios for the variable P_2O_5, which reproduced the statistics and spatial continuity of the initial data. Considering all the scenarios are equally possible representations of the deposit, one of these scenarios was used as a source of information for testing different sampling spacing. Other scenarios can be chosen as a reference for application of the methodology, where the error on the estimate considered in this study, should be similar for different scenarios used as a source of information.

The results showed that a grid of approximately 8m x 8m could be used to produce the acceptable error for the study area (10%). It should be noted that for regions with different variability of P_2O_5 grades the result may be different. Usually the operation uses a spacing of 25m x 25m. According to the results, this spacing is not sufficient to ensure the minimum acceptable error, which means there will be more uncertainty during the planning of the mine, and the block sent to the process plant will have associated error.

The uncertainty magnitude of the estimates depend on the local sampling variability. Clearly, the use of additional information decreases uncertainty and error because the most information available will result in a more precise estimative. Otherwise, more samples mean more money and time spent. The determination of acceptable error and a proper sampling grid is fundamental to mine planning optimization.

ACKNOWLEDGEMENTS

REFERENCES

Li, S., Dimitrakopoulos, R., Scott, J., and Dunn, D., 2004, Quantification of geological uncertainty and risk using stochastic simulation and applications in the coal mining industry, in Orebody Modelling and Strategic Mining Planning: The Australasian Institute of Mining and Metalurgy, Melbourne, p. 233–240.

Koppe, V. C., Costa, J. F. C. L., Peroni, R. L., and Koppe, J. C., 2011. Choosing Between Two Kind of Sampling Patterns Using Geostatistical Simulation: Regularly Spaced or at High Uncertainty Locations? Natural Resources Research.

Emery, X., and Hernández, J., 2009. A geostatistical approach to optimize sampling designs for local forest inventories. Canadian Journal of Forest Research.

Goovaerts, Pierre, 1997. Geostatistics for Natural Resources Evaluation, Oxford University Press, New York.

Matheron, G., 1973. The Intrisic Randon Function and Their Applications. Advances in Applied Probability. V.5. P.439-468.